

Electronic Supplementary Information

**Nanoporous IrO₂ catalyst with enhanced activity and durability
for water oxidation through advancing the micro/meso-pore
structure**

Guoqiang Li,^{a,b,c} Songtao Li,^d Meiling Xiao,^{a,b,c} Junjie Ge,^{*a,b} Changpeng Liu^{a,b} and
Wei Xing^{*a,b}

*Corresponding author: W. Xing, E-mail: xingwei@ciac.ac.cn

J. Ge, E-mail: gejj@ciac.ac.cn

Tel.: 86-431-85262223; Fax: 86-431-85685653

^a State Key Laboratory of Electroanalytical Chemistry, Changchun Institute of Applied Chemistry, Chinese Academy of Sciences, Changchun 130022, PR China.

^b Laboratory of Advanced Power Sources, Jilin Province Key Laboratory of Low Carbon Chemical Power Sources, Changchun Institute of Applied Chemistry, Chinese Academy of Sciences, Changchun 130022, PR China.

^c University of Chinese Academy of Sciences, Beijing 100039, PR China.

^d Institute of Mathematics, Jilin University, Changchun 130012, PR China.

1 Experimental Section

1.1 Preliminary exploration by UV-Vis spectroscopy

UV-Vis spectroscopy characterization was carried out in a Cary 60 spectrophotometer (Agilent Technologies Inc.). Spectra were recorded at room temperature and in a wavelength range between 250 and 600 nm. The effect of two important factors of different proportion and temperature on the reactant H_2IrCl_6 , $\text{NH}_3\cdot\text{H}_2\text{O}$ and NaNO_3 were taken into account during the UV-Vis measurement.

1.2 Exploration by ESI-MS

Based on the results of UV-Vis spectroscopy mentioned above, Electrospray Ionization-Mass Spectrometry (ESI-MS) was applied to further research the intermediate complexes of solution ($n\text{H}_2\text{IrCl}_6 : n\text{NH}_3\cdot\text{H}_2\text{O} = 1:100$): the sample was diluted to 20 μM for immediately MS analysis, then it was analyzed on a LTQ XL linear ion trap mass spectrometer (Thermo, San Jose, CA, USA), which equipped with a conventional ESI source. The sample solution was introduced into ESI-MS by a 250 μL gas-tight syringe (Hamilton, Las Vegas) at a flow rate of 5 $\mu\text{L min}^{-1}$ directly. The sheath gas was set at 35 (arbitrary units). The capillary temperature was set as 250 $^\circ\text{C}$. The capillary voltage and tube lens voltage were set as 25 V and 70 V, respectively. Positive ion mode was used to acquire mass spectrum.

1.3 Synthesis of IrO_2 catalysts

Based on the results from UV-Vis spectroscopy and ESI-MS, several catalysts through intermediates with three degrees of coordination (denoted as IrO_2 (1:100)-450 $^\circ\text{C}$, IrO_2 (1:10)-450 $^\circ\text{C}$ and IrO_2 -450 $^\circ\text{C}$) and through different temperatures (denoted

as IrO₂ (1:100)-400 °C and IrO₂ (1:100)-500 °C) were prepared next.

IrO₂ catalysts were synthesized by an ammonia-induced pore-forming method through heat treatment of intermediate compounds. Firstly, 274.6 mg H₂IrCl₆·xH₂O (35 wt% Ir) was suspended in 40 mL deionized water and then required amounts of NH₃·H₂O with n (H₂IrCl₆·xH₂O) : n (NH₃·H₂O) = 0, 1:10 and 1:100 were added to prepare three types of catalysts, respectively. After the mixture was reacting for 3 h ultrasonically, 4.072 g NaNO₃ was added under stirring and reacting for 1 h. After that, the mixture was heated at 80 °C and magnetically stirred until nearly complete evaporation of water was achieved. The resulting powder was then placed in a quartz boat and heated to 450 °C at a rate of 5 °C min⁻¹, and held for 0.5 h in air. Finally, catalysts denoted as IrO₂ (1:100)-450 °C, IrO₂ (1:10)-450 °C, and IrO₂-450 °C were obtained through filtered and washed with deionized water, respectively, followed by drying at 60 °C in a vacuum oven overnight. Moreover, IrO₂ (1:100)-400 °C and IrO₂ (1:100)-500 °C catalysts were prepared through the same method except for different temperature. Commercial IrO₂ (denoted as IrO₂ (CM), CM is the abbreviation of commercial) catalyst was used for comparison as a baseline catalyst during the linear sweep voltammetry measurement for OER.

1.4 Physical characterization

All X-Ray diffraction (XRD) measurements were performed using a Rigaku-D/MAX-PC2500 X-ray diffractometer (Japan) with the Cu K α (1 λ 1.5405 Å) as a radiation source operating at 40 kV and 200 mA. X-ray photoelectron spectroscopy (XPS) measurements were carried out on a Kratos XSAM-800 spectrometer to determine the

surface electronic structure. The specific surface area and pore size distribution were determined through N₂ gas adsorption/desorption measurements (ASAP 2020, Micromeritics Instrument Corporation, USA). The morphologies of as-prepared samples were characterized with scanning electron microscopy (SEM) measurements performing with an XL 30 ESEM FEG field emission scanning electron microscope, and transmission electron microscopy/ high-resolution transmission electron microscopy (TEM, HRTEM, JEOL JEM-2010) working at an accelerating voltage of 200 kV.

1.5 Electrochemical tests

All electrochemical tests were carried out with a Princeton Applied Research Model273 Potentiostat/Galvanostat and a conventional three electrode electrochemical cell at room temperature with 0.5 mol L⁻¹ H₂SO₄ purged with high-purity N₂ as electrolyte solution. A Pt plate was used as the counter electrode and a saturated calomel electrode (SCE) was used as the reference electrode. However, the potentials in this paper were quoted with respect to reversible hydrogen electrode (RHE). In 0.5 M H₂SO₄, $E(\text{RHE}) = E(\text{SCE}) + 0.26 \text{ V}$. The working electrode was a glassy carbon (GC, 4 mm diameter), it was polished with slurry of 0.3 μm and 0.05 μm alumina successively and washed ultrasonically in deionized water prior to use. The working electrode was prepared as follows: firstly, 5 mg of the catalyst was dispersed ultrasonically in 525 μL solutions containing of 25 μL Nafion® solution (5 wt%) and 0.5 mL alcohol solution; secondly, 5 μL catalyst inks was pipetted and spread on the glassy carbon disk; at last, the electrode was obtained after the solvent

volatilized with the catalyst loading was 0.379 mg cm⁻². Cyclic voltammetry (CV) curves were recorded in a potential window between 0.26 and 1.46 V, and the scanning rate ranged from 2 to 300 mV s⁻¹ in N₂-saturated H₂SO₄ solution at room temperature. The charge (Q) was calculated from the different voltammograms of various scanning rates, by the following equation:

$$Q = \int_{E_1}^{E_2} \frac{|j|}{\nu} dE \quad (1)$$

where j is the current density obtained from CV curves, ν is the scanning rate ranged from 2 to 300 mV s⁻¹, and E is the scanning potential between 0.66 and 1.36 V. The outer charge (Q_O) can be calculated by integrating the voltammogram taken at the scanning rate of 300 mV s⁻¹, which shows the outer and more accessible active surface during OER, while the total charge (Q_T) of the catalysts can be calculated by integrating the same region at a potential scanning rate of 2 mV s⁻¹, which shows the whole active surface for OER.^{1,2} Linear sweep voltammetry (LSV) curves for OER were recorded in a potential window between 1.06 and 1.66 V at a potential scanning rate of 5 mV s⁻¹ in N₂-saturated H₂SO₄ solution at room temperature. The AC impedance spectra were recorded on an Autolab potentiostat in the frequency range of 0.1 Hz to 10 kHz at the potential of 1.56 V, a 10 mV amplitude of sinusoidal potential perturbation was employed in the measurements. The chronoamperometric (CA) experiments were performed in N₂-saturated 0.5 M H₂SO₄ solution at 1.56 V to estimate the performance degradation of the catalysts at room temperature. The accelerated durability tests (ADTs) were performed to assess the catalyst durability by applying cyclic potential sweeps between 1.06 and 1.66 V at a sweep rate of 50 mV/s

for 3000 cycles in N₂-saturated H₂SO₄ solution at room temperature.

Linear sweep voltammetry (LSV) curves for alkaline OER were also carried out to assess the catalytic activities of the as-prepared catalysts. The preparation of working electrode and the counter electrode were same to the acidic test condition, and the reference electrode was Hg/HgO electrode. The potentials reported in our work were vs. the reversible hydrogen electrode (RHE). In 1.0 mol L⁻¹ KOH solution (pH = 14), $E \text{ (RHE)} = E_{\text{Hg/HgO}} + 0.098 + 0.059 \cdot \text{pH}$. The potential window was between 1.06 and 1.66 V at a potential scanning rate of 5 mV s⁻¹ in N₂-saturated 1.0 M KOH solution at room temperature.

1.6 SPEWE cells tests

A Nafion® 115 membrane was used as the solid polymer electrolyte and the pre-treatment of the Nafion® membrane was accomplished by successively treating the membrane in 5 wt% H₂O₂ solution at 80 °C, distilled water at 80 °C, 8 wt% H₂SO₄ solution at 80 °C and then in distilled water at 80 °C again, for 30 min in each step.

Membrane electrode assemblies (MEAs) with 12.5 cm² active cell area were fabricated as follows: Catalyst inks were composed of aqueous dispersions of catalyst, deionized water, Nafion® solution (5 wt%) and isopropyl alcohol. The anode paste was directly deposited onto one side of PTFE membrane by a spray-coating technique, then, it was transferred to the Nafion® 115 membrane by decalomania technique with the catalyst loading was 2.0 mg cm⁻². A Ti mesh (4 cm diameter) was used as the backing layer. A commercial Pt black was used as the catalyst for the H₂ evolution reaction. The cathode paste was spread on carbon paper backings (GDL ELAT from

E-TEK) with the Pt loading of 2.0 mg cm^{-2} . Finally, MEAs were hot pressed at $135 \text{ }^{\circ}\text{C}$ and 5.5 MPa .

Steady state polarization test was performed at $80 \text{ }^{\circ}\text{C}$ in galvanostatic mode using a constant current supply and a single SPEWE cell with an active area of 12.5 cm^2 . Deionized water was pumped into the anode from the water reservoir and was maintained at $80 \text{ }^{\circ}\text{C}$ and atmospheric pressure.

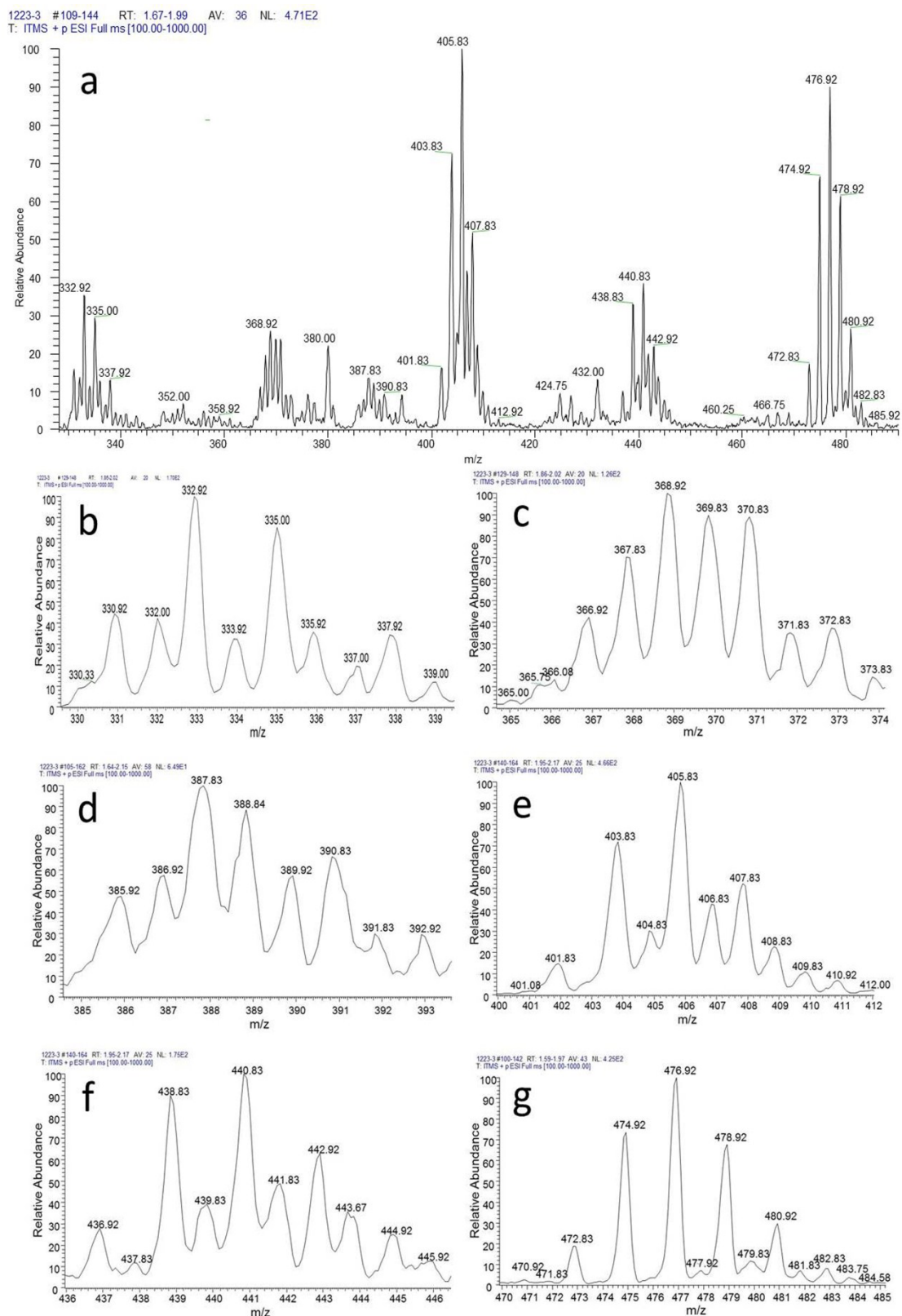


Fig. S1 (a) ESI-MS spectrum of intermediates solution ($\text{nH}_2\text{IrCl}_6 : \text{nNH}_3 \cdot \text{H}_2\text{O} = 1:100$) and (b-g) Isotope peak analyzed from the ESI-MS spectrum.

Table S1. Ion structures and corresponding values analyzed from the ESI-MS spectrum.

serial number	Measured value (<i>m/z</i> ^a)	Ion structures	Theoretical value (<i>m/z</i>)
1	332.92	[Ir(NH ₃)(H ₂ O)Cl ₃] ⁺	332.9045
2	367.83	[HIr(NH ₃) ₂ Cl ₄] ⁺	367.8156
3	368.92	[HIr(NH ₃)(H ₂ O)Cl ₄] ⁺	368.8806
4	369.83	[HIr(H ₂ O) ₂ Cl ₄] ⁺	369.8646
5	387.83	[NH ₄ Ir(NH ₃)(H ₂ O)Cl ₄] ⁺	387.8369
6	388.84	[H ₂ Ir(NH ₃)Cl ₅] ⁺	388.8447
7	405.83	[H(NH ₄)Ir(NH ₃)Cl ₅] ⁺	405.8713
8	406.83	[H ₂ IrCl ₅ (NH ₃ ·H ₂ O)] ⁺	406.8553
9	440.83	[(NH ₄) ₂ IrCl ₅ (NH ₃ ·H ₂ O)] ⁺	440.9083
10	441.83	[H(NH ₄) ₂ IrCl ₆] ⁺	441.8476
11	476.92	[H(NH ₄) ₂ IrCl ₆ (NH ₃ ·H ₂ O)] ⁺	476.8847

^a The isotope peak corresponds to the most intense simulated isotope peak.

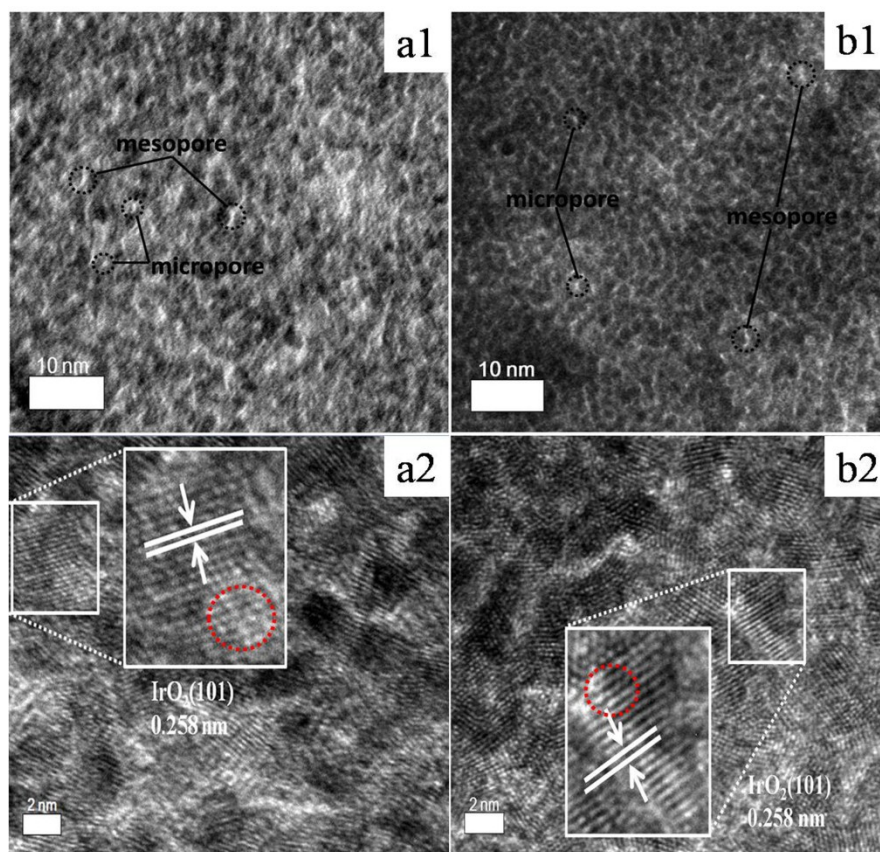


Fig. S2 TEM images and HRTEM images of (a1, a2) IrO₂ (1:100)-400 °C and (b1, b2) IrO₂ (1:100)-500 °C.

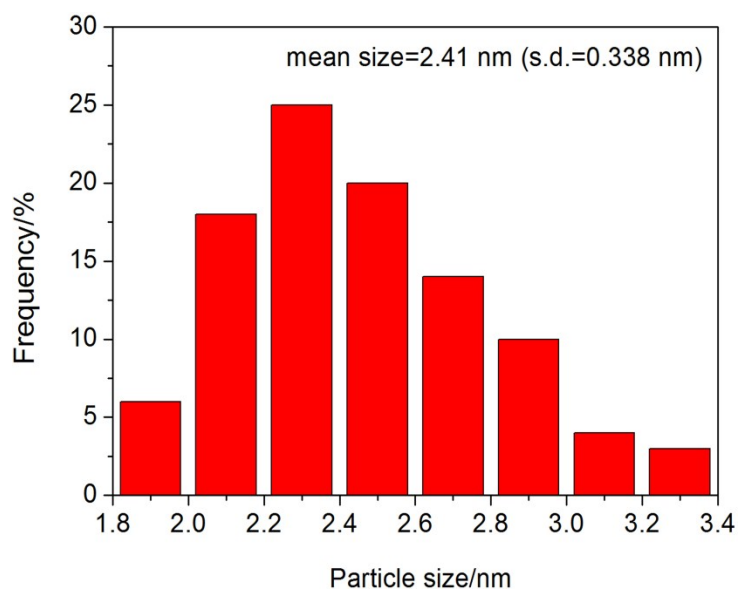


Fig. S3. Particle size distribution histogram of IrO₂ (1:100)-450 °C

The as-obtained data are as follows:

=====Basic report=====

Total 100
 Max./nm 3.36
 Min./nm 1.81
 Mean/nm 2.41
 No. Particle size/nm

1	1.82
2	2.42
3	1.82
4	2.22
5	2.53
6	1.81
7	2.81
8	3.12
9	1.81
10	2.10
11	2.72
12	2.08
13	1.88
14	1.87
15	2.01
16	2.09
17	2.61
18	3.36
19	3.02
20	2.11

21 2.07
22 2.03
23 2.61
24 2.84
25 2.67
26 2.47
27 2.12
28 2.05
29 2.20
30 2.04
31 2.42
32 2.13
33 2.11
34 2.47
35 2.28
36 2.42
37 2.07
38 2.02
39 2.02
40 2.50
41 2.62
42 2.11
43 2.21
44 2.21
45 2.28
46 2.29
47 2.21
48 2.81
49 2.88
50 2.25
51 2.21
52 2.42
53 2.30
54 2.22
55 2.31
56 2.44
57 2.51
58 2.22
59 2.25
60 2.21
61 2.23
62 2.33
63 2.70
64 2.25

65 2.32
 66 2.53
 67 2.33
 68 2.23
 69 2.23
 70 2.53
 71 2.29
 72 2.22
 73 2.22
 74 2.42
 75 3.02
 76 2.12
 77 2.43
 78 2.52
 79 2.42
 80 2.51
 81 2.69
 82 2.41
 83 2.51
 84 2.48
 85 2.62
 86 2.71
 87 2.68
 88 2.63
 89 2.63
 90 2.72
 91 2.62
 92 3.23
 93 2.81
 94 2.90
 95 2.82
 96 2.82
 97 2.86
 98 2.81
 99 3.22
 100 3.05

=====Statistical report=====

Distr./nm	Mean/nm	Amount	Freq.
1.8-2.0	1.9	6	0.060
2.0-2.2	2.1	18	0.180
2.2-2.4	2.3	25	0.250
2.4-2.6	2.5	20	0.200
2.6-2.8	2.7	14	0.140
2.8-3.0	2.9	10	0.100

3.0-3.2	3.1	4	0.040
3.2-3.4	3.3	3	0.030

Based on the sizes of the corresponding 100 nanoparticles, the standard deviation of 0.338 nm can be obtained.

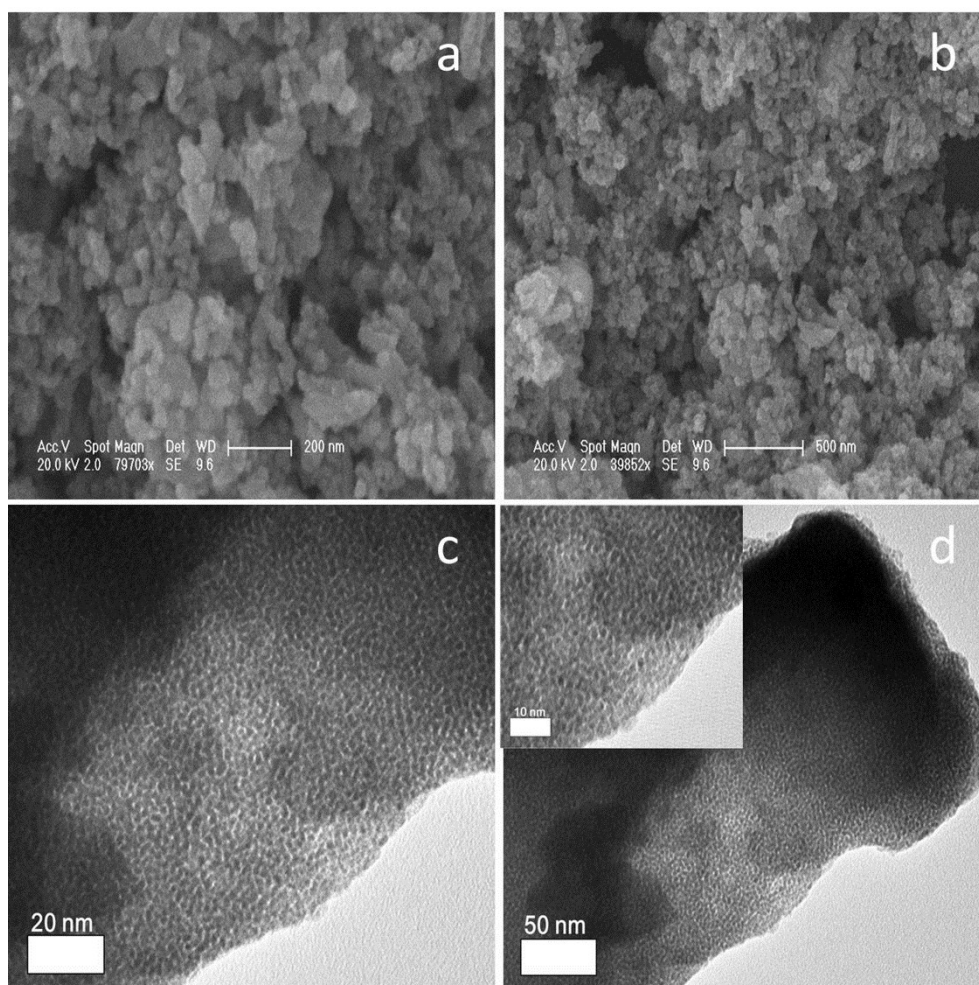


Fig. S4 (a, b) SEM images and (c, d) TEM images IrO₂ (1:100)-450 °C.

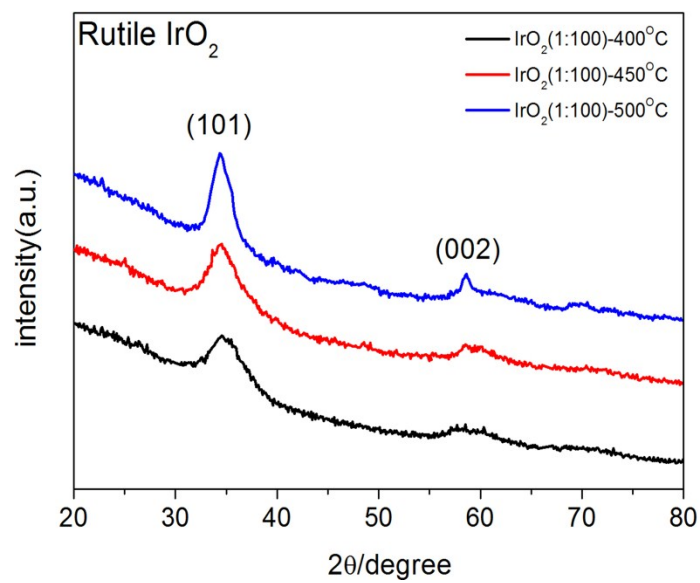


Fig. S5 XRD patterns of IrO_2 (1:100)-400 °C, IrO_2 (1:100)-450 °C and IrO_2 (1:100)-500 °C.

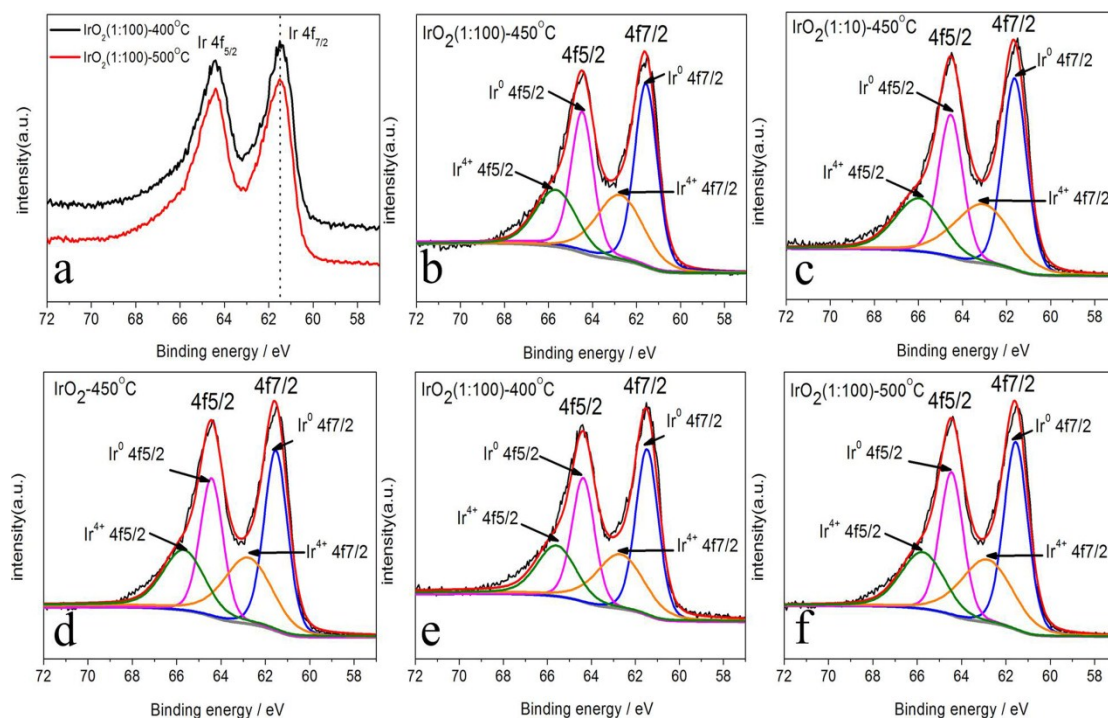


Fig. S6 (a) Ir 4f XPS spectra and (e, f) Fitting curves of Ir 4f XPS spectra of IrO₂ (1:100)-400 °C and IrO₂ (1:100)-500 °C. (b-d) Fitting curves of Ir 4f XPS spectra of IrO₂ (1:100)-450 °C, IrO₂ (1:10)-450 °C and IrO₂-450 °C.

Table S2. XPS analysis of IrO₂ (1:100)-450 °C, IrO₂ (1:10)-450 °C, IrO₂-450 °C, IrO₂ (1:100)-400 °C and IrO₂ (1:100)-500 °C.

Catalyst	Ir 4f7/2		
	Assignment	Position (eV)	Intensity (%)
IrO ₂ (1:100)-450 °C	Ir ⁰	61.5	58.2
	Ir ⁴⁺	62.7	41.8
IrO ₂ (1:10)-450 °C	Ir ⁰	61.6	57.5
	Ir ⁴⁺	63.0	42.5
IrO ₂ -450 °C	Ir ⁰	61.5	54.8
	Ir ⁴⁺	62.8	45.2
IrO ₂ (1:100)-400 °C	Ir ⁰	61.5	56.8
	Ir ⁴⁺	62.7	43.2
IrO ₂ (1:100)-500 °C	Ir ⁰	61.6	57.6
	Ir ⁴⁺	62.9	42.4

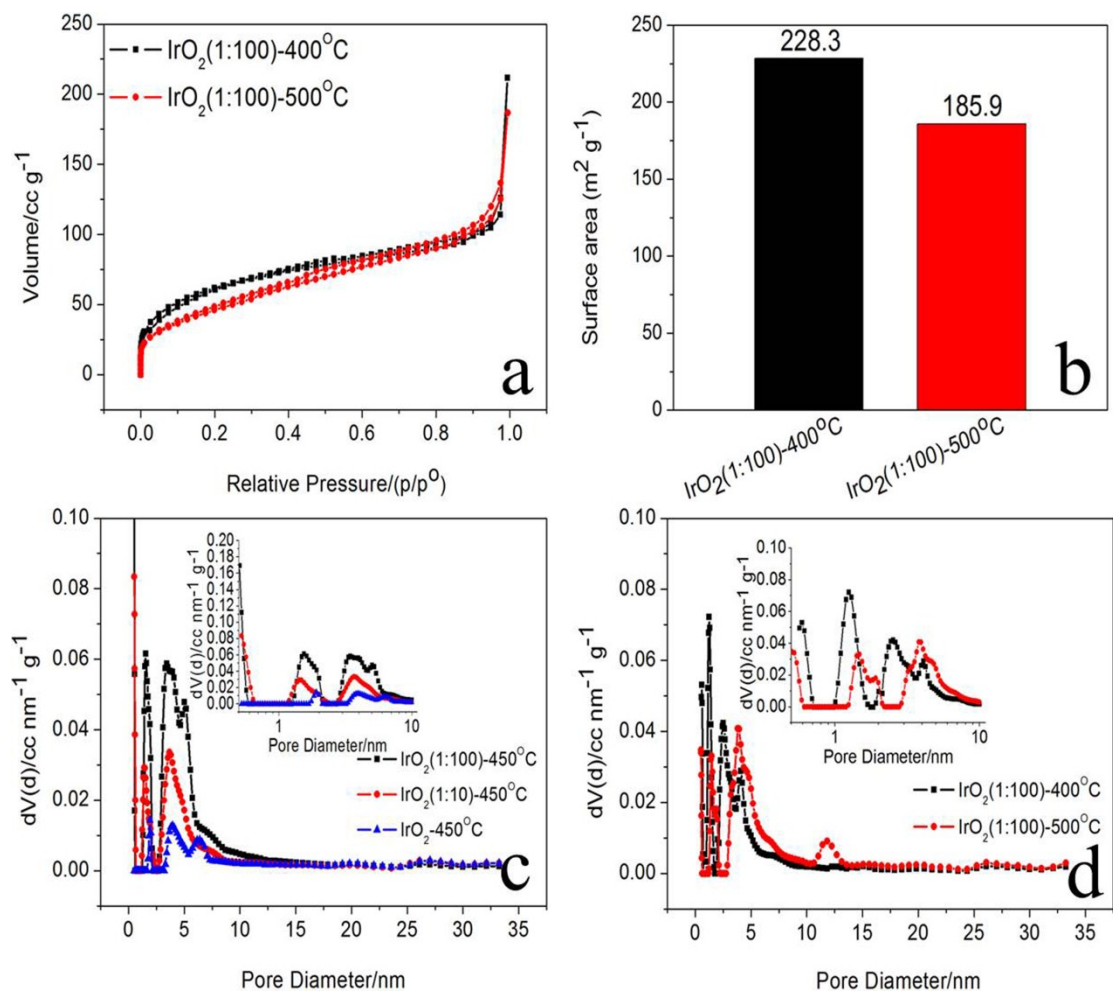


Fig. S7 (a) N₂ adsorption/desorption isotherms, (b) BET specific surface areas, and (d) Corresponding DFT pore-size distribution analyzed from the desorption branch of IrO₂ (1:100)-400 °C and IrO₂ (1:100)-500 °C. (c) Corresponding DFT pore-size distribution analyzed from the desorption branch of IrO₂ (1:100)-450 °C, IrO₂ (1:10)-450 °C and IrO₂-450 °C.

Table S3. Pore volume and Pore-size distribution analyzed from the desorption branch of IrO₂ (1:100)-450 °C, IrO₂ (1:10)-450 °C, IrO₂-450 °C, IrO₂ (1:100)-400 °C and IrO₂ (1:100)-500 °C.

Catalyst	Pore volume (cc g ⁻¹)	0-2 nm	Percentage (%)	2-35 nm	Percentage (%)
IrO ₂ (1:100)-450 °C	0.290	0.06946	29.3	0.16756	70.7
IrO ₂ (1:10)-450 °C	0.163	0.02809	24.9	0.0848	75.1
IrO ₂ -450 °C	0.075	0.00681	7.3	0.08618	92.7
IrO ₂ (1:100)-400 °C	0.208	0.03254	26.1	0.0919	73.9
IrO ₂ (1:100)-500 °C	0.229	0.02251	18.6	0.09823	81.4

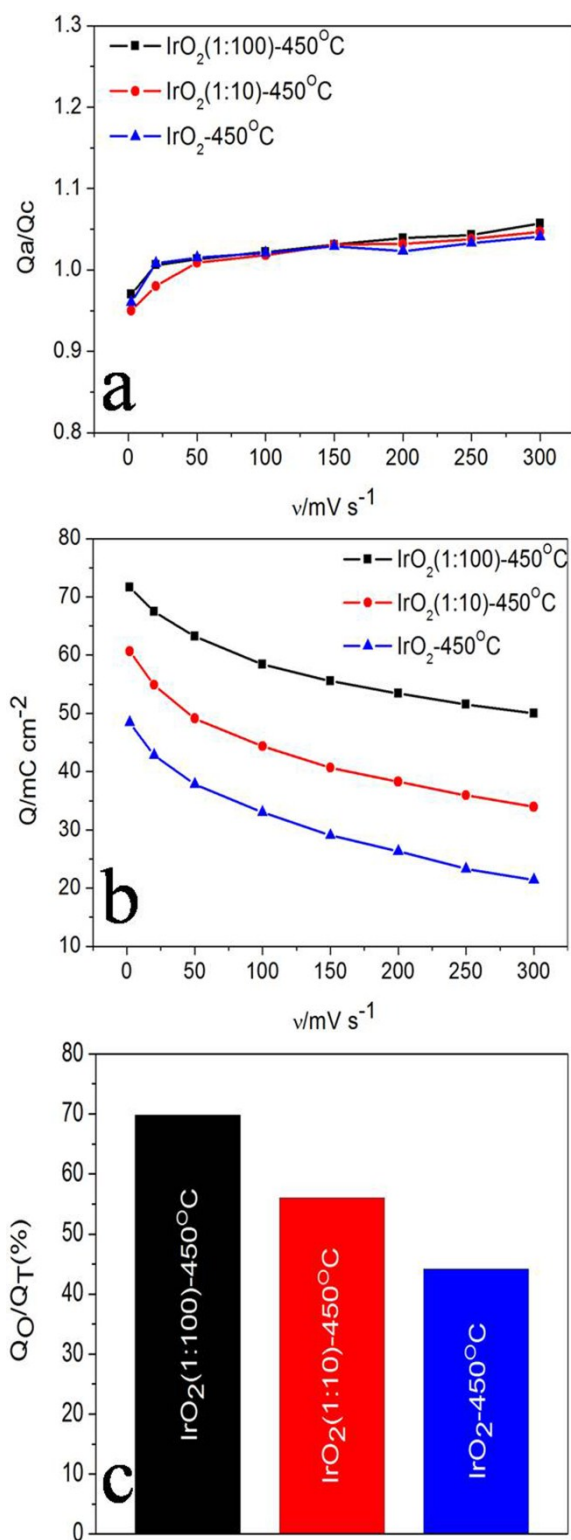


Fig. S8 (a) The reversibility of redox and charging process, (b) Dependence of the voltammetric charges Q_a on the scanning rates of 2-300 mV s^{-1} , and (c) The ratios of outer charge to total charge at the scanning rates of 300 and 2 mV s^{-1} of $\text{IrO}_2(1:100)\text{-}450^\circ\text{C}$, $\text{IrO}_2(1:10)\text{-}450^\circ\text{C}$ and $\text{IrO}_2\text{-}450^\circ\text{C}$ in N_2 saturated 0.5 M H_2SO_4 at room temperature. Catalyst loading: 0.379 mg cm^{-2} .

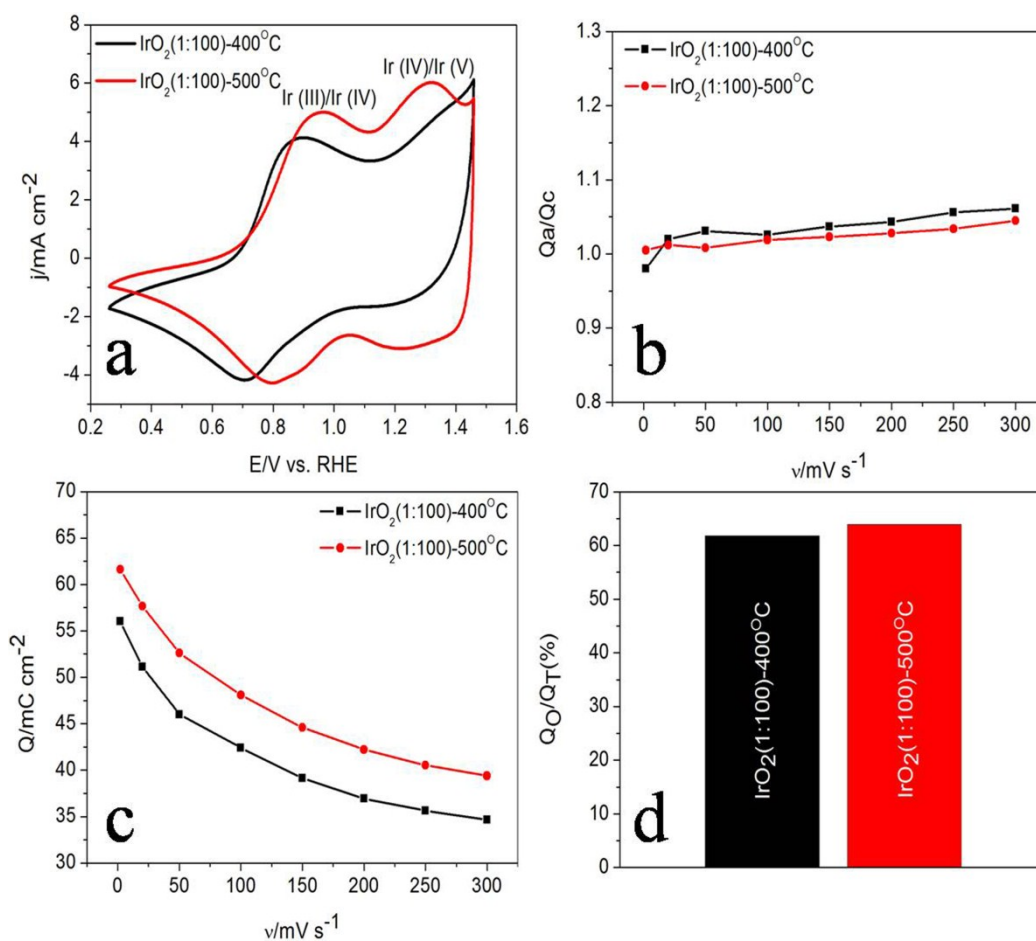


Fig. S9 (a) Cyclic voltammograms at the scanning rate of 50 mV s⁻¹, (b) The reversibility of redox and charging process, (c) Dependence of the voltammetric charges on the scanning rates of 2-300 mV s⁻¹, and (d) The ratios of outer charge to total charge at the scanning rates of 300 and 2 mV s⁻¹ of IrO₂ (1:100)-400 °C and IrO₂ (1:100)-500 °C in N₂ saturated 0.5 M H₂SO₄ at room temperature. Catalyst loading: 0.379 mg cm⁻².

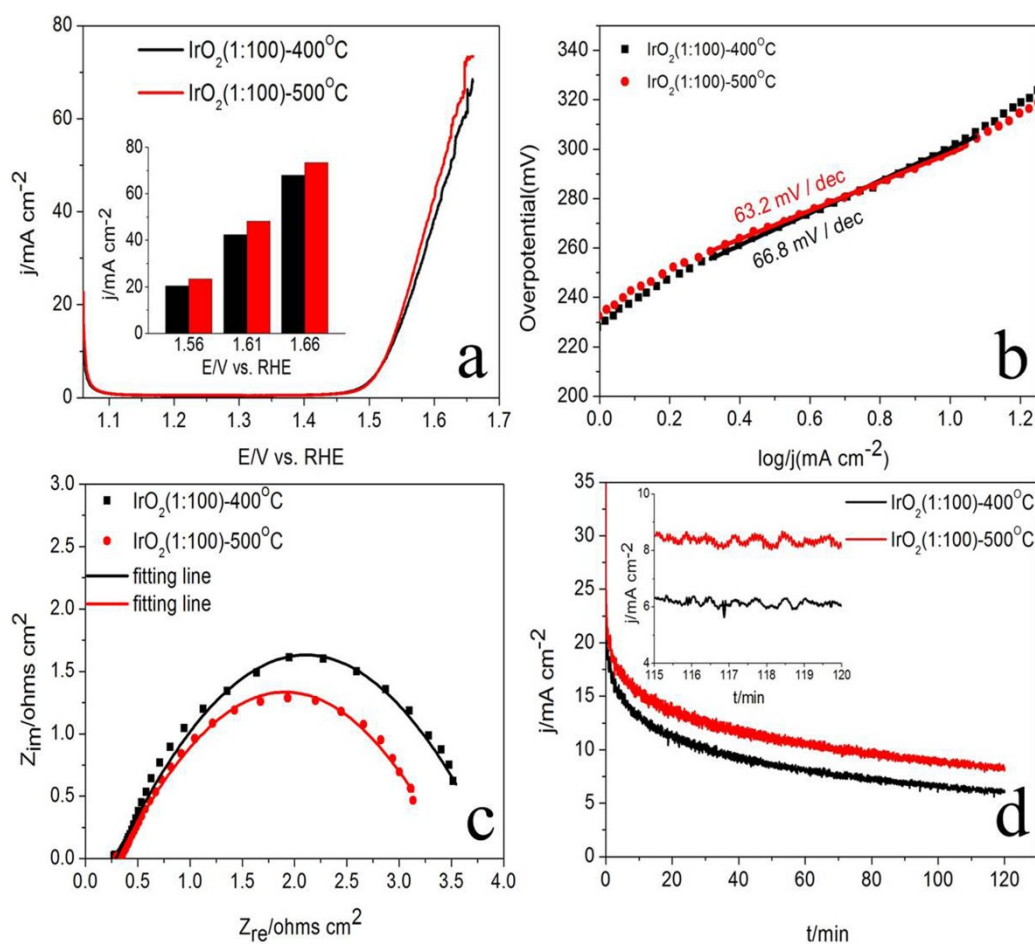


Fig. S10 (a) Linear sweep voltammetry curves (the inset shows the current densities at different applied voltages) at the scanning rate of 5 mV s^{-1} , (b) Tafel plots for OER, (c) AC impedance spectra at 1.56 V in a sweeping frequency range from 0.1 Hz to 10 kHz with an alternate signal of 10 mV, and (d) Chronoamperometric experiments under a constant polarization potential of 1.56 V in N₂ saturated 0.5 M H₂SO₄ at room temperature. Catalyst loading: 0.379 mg cm^{-2} .

Table S4. Electrocatalytic analysis of linear sweep voltammetry curves in 0.5 M H₂SO₄ solution.

Catalyst	Overpotential/10 mA cm ⁻²
IrO ₂ (1:100)-450 °C	282 mV
IrO ₂ (1:10)-450 °C	300 mV
IrO ₂ -450 °C	312 mV
IrO ₂ (1:100)-400 °C	301 mV
IrO ₂ (1:100)-500 °C	299 mV
IrO ₂ (CM)	321 mV

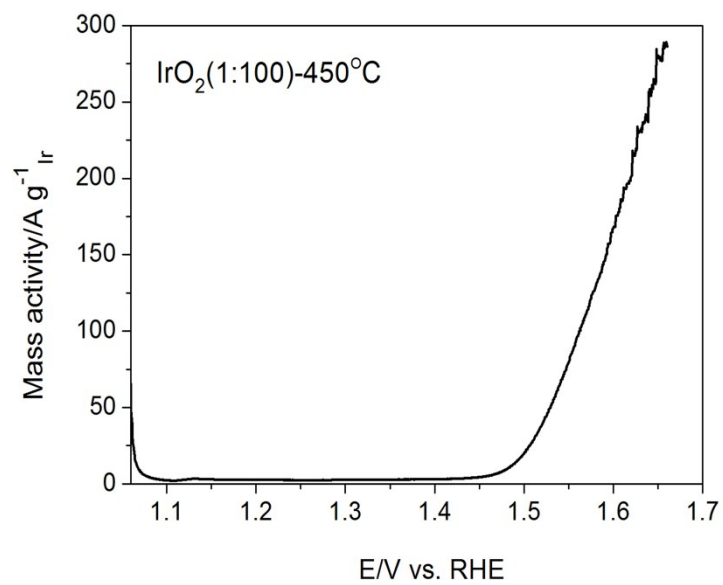


Fig. S11 Mass activity of IrO₂ (1:100)-450 °C catalyst at the scanning rate of 5 mV s⁻¹ in N₂ saturated 0.5 M H₂SO₄ at room temperature. Catalyst loading: 0.379 mg cm⁻².

Table S5. Comparison of OER mass activity for IrO₂ (1:100)-450 °C with other electrocatalysts in acidic media.

Catalyst	Loading	Electrolytes	Scan rate (mV s ⁻¹)	Potential (V)	Mass activity	References
IrO ₂ (1:100)- 450 °C	0.379 mg _{IrO₂} cm ⁻²	0.5 M H ₂ SO ₄	5	1.48	9.6 A g ⁻¹ _{Ir}	This work
				1.51	28.5 A g ⁻¹ _{Ir}	
				1.55	80.3 A g ⁻¹ _{Ir}	
Ir/Ti ₄ O ₇	0.160 mg _{Ir/Ti₄O₇} cm ⁻²	0.5 M H ₂ SO ₄	5	1.48	4.2 A g ⁻¹ _{Ir}	3
IrO _x -Ir	0.133 mg _{IrO_x-Ir} cm ⁻²	0.5 M H ₂ SO ₄	5	1.48	8 A g ⁻¹ _{oxide}	4
IrO _x /C					~35 A g ⁻¹ _{Ir}	5
IrO _x /com.-ATO	10.2 μg _{Ir} cm ⁻²	0.05 M H ₂ SO ₄	5	1.51	~30 A g ⁻¹ _{Ir}	
IrNiO _x (180- 400°C)					>50 A g ⁻¹ _{Ir}	
IrNiO _x (500°C)					~25 A g ⁻¹ _{Ir}	
Ir/TiO ₂	17.8 μg _{Ir} cm ⁻²	0.1 M HClO ₄	20	1.55	70 A g ⁻¹ _{Ir}	6
Ir, IrO ₂ , Ir/Vulcan					≥140 A g ⁻¹ _{Ir}	

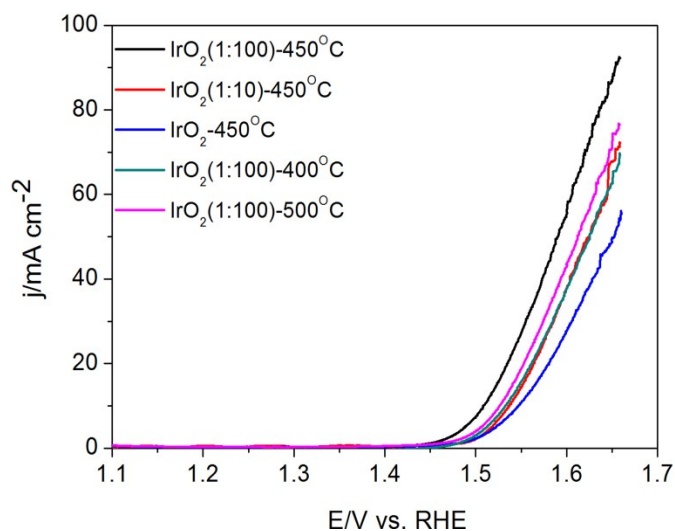


Fig. S12 Linear sweep voltammetry curves at the scanning rate of 5 mV s^{-1} in N_2 saturated 1.0 M KOH at room temperature. Catalyst loading: 0.379 mg cm^{-2} .

Table S6. Electrocatalytic analysis of linear sweep voltammetry curves in 1.0 M KOH solution.

Catalyst	Overpotential/ 10 mA cm^{-2}
$\text{IrO}_2 (1:100)\text{-}450 \text{ }^\circ\text{C}$	276 mV
$\text{IrO}_2 (1:10)\text{-}450 \text{ }^\circ\text{C}$	303 mV
$\text{IrO}_2\text{-}450 \text{ }^\circ\text{C}$	313 mV
$\text{IrO}_2 (1:100)\text{-}400 \text{ }^\circ\text{C}$	300 mV
$\text{IrO}_2 (1:100)\text{-}500 \text{ }^\circ\text{C}$	294 mV

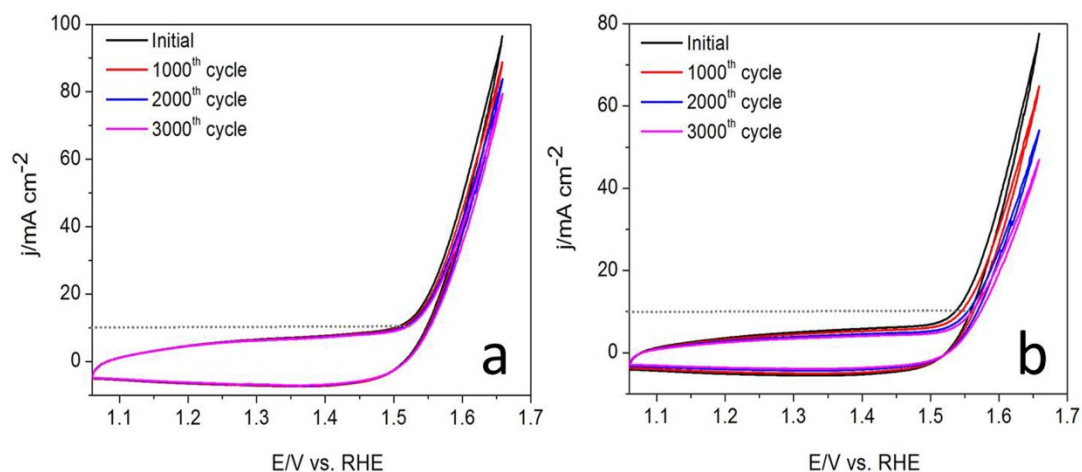


Fig. S13 Cyclic voltammograms of accelerated durability tests by applying cyclic potential sweeps between 1.06 and 1.66 V at a sweep rate of 50 mV/s for 3000 cycles in N₂ saturated 0.5 M H₂SO₄ at room temperature. (a) IrO₂ (1:100)-450 °C and (b) IrO₂-450 °C catalysts. Catalyst loading: 0.379 mg cm⁻².

References

1. A. Marshall, B. Borresen, G. Hagen, M. Tsykin and R. Tunold, *Electrochim. Acta.*, 2006, **51**, 3161-3167.
2. S. Ardizzone, G. Fregonara and S. Trasatti, *Electrochim. Acta.*, 1990, **35**, 263-267.
3. L. Wang, P. Lettenmeier, U. Golla-Schindler, P. Gazdzicki, N. A. Canas, T. Morawietz, R. Hiesgen, S. S. Hosseiny, A. S. Gago and K. A. Friedrich, *Phys. Chem. Chem. Phys.*, 2016, **18**, 4487-4495.
4. P. Lettenmeier, L. Wang, U. Golla-Schindler, P. Gazdzicki, N. A. Canas, M. Handl, R. Hiesgen, S. S. Hosseiny, A. S. Gago and K. A. Friedrich, *Angew. Chem.*, 2016, **128**, 752-756.
5. H. N. Nong, H-S. Oh, T. Reier, E. Willinger, M-G. Willinger, V. Petkov, D. Teschner and P. Strasser, *Angew. Chem. Int. Ed.*, 2015, **54**, 2975-2979.
6. S. M. Alia, B. Rasimick, C. Ngo, K. C. Neyerlin, S. S. Kocha, S. Pylypenko, H. Xu and B. S. Pivovar, *J. Electrochem. Soc.*, 2016, **163**, F3105-F3102.